Reductive Amination of Oxidized Hydroxypropyl Cellulose with ω-Aminoalkanoic Acids as an Efficient Route to Zwitterionic Derivatives

Yang Zhou *[a,c,e], Yimin Yao [b,c], Zhenghao Zhai [c], Mennatallah A. Mohamed [d], Fiorella Mazzini [a,c], Qingqing Qi [d], Michael J. Bortner [b,c], Lynne S. Taylor [d], Kevin J. Edgar [a,c]

[a] *Department of Sustainable Biomaterials, Virginia Tech, Blacksburg, VA 24061, United States*

[b] *Department of Chemical Engineering, Virginia Tech, Blacksburg, VA 24061, United States*

[c] *Macromolecules Innovation Institute, Virginia Tech, Blacksburg, VA 24061, United States*

[d] *Department of Industrial and Physical Pharmacy, Purdue University, West Lafayette, IN 47907, United States*

[e] *Division of Chemistry and Chemical Engineering, California Institute of Technology, Pasadena, CA 91125, United States*

**Corresponding author. E-mail: zhouyang@vt.edu*

Abstract

Zwitterionic polymers, with their equal amounts of cationic and anionic functional groups, have found widespread utility including as non-fouling coatings, hydrogel materials, stabilizers, antifreeze materials, and drug carriers. Polysaccharide-derived zwitterionic polymers are attractive because of their sustainable origin, potential for lower toxicity, and possible biodegradability, but previous methods for synthesis of zwitterionic polysaccharide derivatives have been limited in terms of flexibility and attainable degree of substitution (DS) of charged entities. We report herein successful design and synthesis of zwitterionic polysaccharide derivatives, in this case based on cellulose, by reductive amination of oxidized 2-hydroxypropyl cellulose (Ox-HPC) with ω-aminoalkanoic acids. Reductive amination products could be readily obtained with DS(cation) (= DS(anion)) up to 1.6. Adduct hydrophilic/hydrophobic balance (amphiphilicity) can be influenced by selecting the appropriate chain length of the ω-aminoalkanoic acid. This strategy is shown to

produce a range of amphiphilic, water-soluble, moderately high glass transition temperature (T_g) polysaccharide derivatives in just a couple of efficient steps from commercially available building blocks. The adducts were evaluated as crystallization inhibitors. They are strong inhibitors of crystallization even for the challenging, poorly soluble, fast-crystallizing prostate cancer drug enzalutamide, as supported by surface tension and Flory–Huggins interaction parameter results.

Keywords: Cellulose, zwitterionic polymers, ω-aminoalkanoic acids, amphiphilicity

1. Introduction

Zwitterionic polymers are unusual in that they possess, by definition, both cationic and anionic functional groups (Harijan & Singh, 2022); therefore they may exhibit properties characteristic of both ionic and nonionic polymers (Laschewsky & Rosenhahn, 2018). Zwitterionic polymers have shown particular utility as non-fouling coatings, addressing important problems including that of marine biofouling (Cheng et al., 2009; Wang et al., 2015). They also have value in hydrogels (Haag & Bernards, 2017), as stabilizers (Rodriguez et al., 2018), as antifreeze materials (Matsumura & Hyon, 2009), and as carriers for drugs (Blackman, Gunatillake, Cass, & Locock, 2019; Shen, Akagi, & Akashi, 2012). Polymers with both positively and negatively charged groups include polyampholytes and polyzwitterions. Unlike polyampholytes, which may contain different numbers of anionic and cationic groups (and their associated counterions), polyzwitterions have equal numbers of positively and negatively charged groups, even at nanometer length scale under certain conditions (Laschewsky, 2014; Laschewsky et al., 2018). Polyzwitterions are typically quite responsive to external environmental stimuli, including pH, temperature, and salt concentration (Blackman et al., 2019). There have historically been two categories of approaches to zwitterionic polymer synthesis: direct polymerization of zwitterionic monomers, and post-polymerization modification to introduce zwitterionic moieties (Zheng, Sundaram, Wei, Li, & Yuan, 2017). Direct polymerization frequently involves protection and deprotection steps, since the unprotected ionic functionality may not be compatible with the chosen polymerization technique (Blackman et al., 2019). Post-polymerization introduction of ionic or zwitterionic groups can be an alternative to painstaking direct polymerization processes. However, it is generally difficult to achieve the desired content of zwitterionic groups. This may be due to restricted approach angles, repulsion between like charges, and/or slow diffusion of the polymeric

substrate (Blackman et al., 2019; Zheng, Sun, et al., 2017). Sulfobetaines (SB), carboxybetaines (CB), and phosphorylcholines (PC) are among the zwitterionic groups commonly introduced to polymers to impart zwitterionic character (Debayle et al., 2019).

Natural zwitterionic polysaccharides have been identified from bacteria (Tzianabos, Wang, & Kasper, 2003). Synthetic polysaccharide-based polymers have also attracted significant interest (Elschner et al., 2016; Gabriel, Gericke, & Heinze, 2019; Zheng, Sun, et al., 2017). However, the low aqueous solubility of the most abundant, commercially significant polysaccharides including cellulose, chitosan, and starch restricts the approaches available for synthesis of zwitterionic polysaccharide derivatives (Zheng, Sun, et al., 2017). Some of the zwitterionic polysaccharide derivatives that have been prepared had only low degree of substitution (DS) (< or << 1) of the charged moieties (Calabrese et al., 2018; Haro-Mares et al., 2020; Laureano-Anzaldo, Robledo-Ortíz, & Manríquez-González, 2021; Liu, Liu, Esker, & Edgar, 2016; Zeng et al., 2012), or bore an overall net charge (so were not truly zwitterionic) (Calabrese et al., 2018; Laureano-Anzaldo et al., 2021). The DS of charged entities in a polymer can substantially influence its physical and chemical properties.

Hydroxypropyl cellulose (HPC), which has broad solubility including in water and several organic solvents, is a derivative of natural cellulose that has widespread commercial applications. It is made by condensation of cellulose and propylene oxide in aqueous alkaline media, providing cellulose ethers that have oligo(hydroxypropyl) substituents, each of which is terminated by a secondary alcohol (Arca et al., 2018). Among its other uses, this polymer made from renewable cellulose finds use in amorphous solid dispersions for enhancing drug solubility and bioavailability (Dong, Mosquera-Giraldo, Troutman, et al., 2016), as well as in targeted drug and gene delivery systems (Ganta, Devalapally, Shahiwala, & Amiji, 2008). Recently, the Edgar group discovered that the presence of terminal secondary alcohols of the HPC oligo(hydroxypropyl) substituents, with their wider approach angles than those of anhydroglucose ring hydroxyls, can be exploited for regioselective oxidation. In particular, treatment of HPC with simple household bleach (NaOCl) oxidizes those secondary alcohols to ketones with remarkable regioselectivity, introducing moieties that are amenable to further modification (Nichols, Chen, Mischnick, & Edgar, 2020; Stevens, Chapman, & Weller, 1980) including for conversion to all-polysaccharide hydrogels by reaction with polyfunctional amine-containing polymers (Chen, Nichols, Norris, Frazier, & Edgar, 2020). This reaction requires neither protecting groups for the introduced ketones, nor does it

cleave monosaccharide rings (introducing instability, reducing degree of polymerization (DP), and impacting physical properties), as does the commonly employed periodate oxidation (Amer et al., 2016; Strätz, Liedmann, Heinze, Fischer, & Groth, 2020). It struck us that these newly introduced ketone groups could be attractive sites for introducing zwitterionic groups by a post-polymerization approach. In particular, we made note of the fact that ω-aminoalkanoic acids are commercially available, relatively inexpensive materials. Several ω-aminoalkanoic acids are used in vast amounts as monomers, producing polymers including nylons and polyesters (Song, Lee, Bornscheuer, & Park, 2014). The shortest ω-aminoalkanoic acid is actually the natural amino acid glycine ($H_2NCH_2CO_2H$). These could be attractive reagents for our purposes, not least because they might permit simultaneous introduction of the cation and anion, ensuring charge neutrality and true zwitterionic character under near-neutral environmental conditions, such as those that exist in normal cells, in circulation, or in the human small and large intestines (Elschner et al., 2016). This is a potentially appealing new route to poly(zwitterionic) polysaccharides that might bring biodegradability, renewability, and lower toxicity to traditional zwitterionic polymer applications. In addition, these zwitterionic polysaccharides also promise to be amphiphilic materials with improved water solubility, thereby making them potentially attractive candidates as amorphous solid dispersion polymers (Liu, Taylor, & Edgar, 2015).

We hypothesize that a simple two-step strategy could be effective for synthesis of zwitterionic cellulose derivatives: (1) regioselective oxidation of the terminal hydroxyl of HPC to introduce ketone groups, and (2) reductive amination of these ketones with ω-aminoalkanoic acids. We predict that the DS(zwitterions) (hereafter we use the general term DS(Zw)) should be highly controllable by this approach, since the oligo(hydroxypropyl) termini are flexible and have wide approach angles. We further hypothesize that amphiphilic, poly(zwitterionic) polysaccharide derivatives will be effective stabilizers against crystallization of hydrophobic drug actives, and display surface activity. Herein we describe attempts to use this approach to synthesize a range of zwitterionic polymers that vary in ω-aminoalkanoate side chain length, and investigations of their properties, including thermal stability, solubility, drug release enhancement and crystallization inhibition, and surface activity. It is important to note that referring the products as “zwitterionic polymers” indicates their potential to exist in zwitterionic form under specific circumstances (e.g., at neutral pH); at extremes of pH, the zwitterionic character can be lost.

2. Methods and materials

HPC was purchased from Acros Organics and used as received (average M.W. 100,000 g/mol (as reported by manufacturer); molar substitution (MS) and DS of HP 4.7 and 2.3, respectively (see ^{1}H NMR method description below)). Glycine (≥ 99%), 4-aminobutyric acid (γ-aminobutyric acid, ≥ 99%), 5-aminovaleric acid (97%), 6-aminohexanoic acid, and sodium cyanoborohydride were purchased from Sigma-Aldrich. Spectra/Por 7 dialysis membranes (MWCO 3.5 K) were purchased from Thermo Fisher Scientific. Enzalutamide was purchased from ChemShuttle (Hayward, California). All samples for Fourier transform infrared spectroscopy (FTIR), thermogravimetric analysis (TGA), and differential scanning calorimetry (DSC) were dried at 80 °C under vacuum overnight.

2.1. Measurements

^{1}H, ^{13}C, ^{1}H–^{1}H COSY, and ^{1}H–^{13}C HSQC NMR spectra were acquired on either Bruker Avance 500 or 600 MHz spectrometers. Samples were analyzed as solutions in D_2O at 25 °C in standard 5 mm o.d. tubes. ^{1}H NMR spectra were referenced to D_2O (4.79 ppm). ^{13}C NMR spectra were referenced to 3-(trimethylsilyl)propionic-2,2,3,3-*d*$_4$ acid, sodium salt (0 ppm). Attenuated total reflectance sampling FTIR (ATR-FTIR) was performed with a Nicolet iS50 spectrometer. TGA was performed using a TA Instruments Q5500 under nitrogen. Samples were equilibrated at 30 °C and ramped to 800 °C with a heating rate of 10 °C/min under nitrogen. DSC was carried out using a TA Instrument Q2000. Each sample was loaded into an individual Tzero aluminum pan. Samples were subjected to a heat/cool/heat cycle between -50 °C and 180 °C under nitrogen purge at heating and cooling rates of 10 °C/min. Second heating scans were used to determine T_g.

2.2. HPC MS and DS determination

MS(HP) was calculated by ^{1}H NMR spectroscopy in D_2O from the ratio of HPC methyl and backbone proton integrals. DS(HP) was determined from the ratio of terminal (1.09 ppm) to internal (0.94 ppm) methyl group integrals. Carbanilation of HPC hydroxyl groups was employed to shift the terminal methyl resonances downfield (method modified from (Arca, Mosquera-Giraldo, Taylor, & Edgar, 2017; Dong, Mosquera-Giraldo, Troutman, et al., 2016)). Measured values: DS(HP) 2.3, MS(HP) 4.7.

2.3. Determination of DS(ketone) of Ox-HPC and DS(Zw) of HPC-AA1, HPC-AA3, HPC-AA4, and HPC-AA5

DS(ketone) was determined by ^{1}H NMR spectroscopy **(Figure 1)**.

$$\frac{\mathrm{I(a'')}}{\mathrm{I(a\ \&\ a') + I(a'')}} = \frac{\mathrm{DS(ketone)}}{\mathrm{MS(HP)}} \quad (1)$$

Letters correspond to those of Ox-HPC in **Figure 1**. In the equation, **a** refers to methyl protons of internal hydroxypropyl monomers; the letter **a'** refers to methyl protons of the terminal hydroxypropyl group on oligomers where no oxidation has occurred; the letter **a"** refers to methyl protons of the terminal hydroxypropyl group that has been oxidized to a ketone.

DS(Zw) was determined by ^{1}H NMR spectroscopy **(Figure 1)**.

For HPC-AA1:

$$\frac{\mathrm{I(a'')}}{\mathrm{I(a\ \&\ a') + I(a'')}} = \frac{\mathrm{DS(Zw)}}{\mathrm{MS(HP)}} \quad (2)$$

Letters correspond to those of HPC-AA1. Letter **a** refers to methyl protons of internal hydroxypropyl monomers; **a'** refers to methyl protons of the terminal hydroxypropyl group on oligomers where no oxidation has occurred; **a''** refers to methyl protons of the terminal hydroxypropyl group that bears an amine substituent. The overlapped resonances a'' and (a and a') were deconvoluted using the *Gaussian LorenCross* function.

For HPC-AA3, HPC-AA4, and HPC-AA5:

$$\frac{\mathrm{I(CH_2\ next\ to\ carboxyl\ group)}}{\mathrm{I(a\ \&\ a') + I(a'')}} = \frac{2 \times \mathrm{DS(Zw)}}{3 \times \mathrm{MS(HP)}} \quad (3)$$

Letters correspond to those of HPC-AA3, HPC-AA4, and HPC-AA5 in **Figure 1**. Letter **a** refers to methyl protons of internal hydroxypropyl monomers; **a'** refers to methyl protons of the terminal hydroxypropyl group on oligomers where no oxidation has occurred; **a"** refers to methyl protons of the terminal hydroxypropyl group that bears an amine substituent. "CH_2 next to carboxyl group" means: **f** for HPC-AA3, **g** for HPC-AA4, or **h** for HPC-AA5.

2.4. Synthesis of Ox-HPC

The method was adapted from that of (Nichols et al., 2020; Zhou, Zhai, et al., 2022). HPC (8 g, 18.4 mmol) was dissolved in DI water (100 mL) in a 1000 mL round-bottom flask. Acetic acid (10 mL, 174.8 mmol, 9.5 equiv. per AGU) was added to the NaOCl aqueous solution (100 mL, 366.7 mmol, 19.9 equiv. per AGU) dropwise in an ice bath. Then, the mixture was added to the round-bottom flask dropwise with vigorous stirring using ice bath cooling. The solution then was kept at RT with stirring for 12 h. Isopropyl alcohol (16 mL, 209.3 mmol, 11.4 equiv. per AGU) was added and the solution stirred 30 min to consume any residual hypochlorite. Then the mixture was poured into a 2000 mL beaker. Aqueous sodium carbonate (140 mL 20% (w:v) Na_2CO_3, 264.2 mmol, 14.4 equiv. per AGU) was added to the beaker dropwise with stirring using a cool water bath, then the mixture was stirred at RT for 1 h. The reaction mixture was then dialyzed against DI water for 6 days. The final product was collected by freeze-drying as a white fibrous material (4.60 g, yield 58%, DS(ketone): 1.8). ^{1}H NMR (500 MHz, D_2O): 1.15 ($C\underline{H}_3$–CH(–OH)–CH_2–O– and (–O–CH(–$C\underline{H}_3$)–CH_2–)$_n$ in side chains), 2.15 ($C\underline{H}_3$–C(=O)–CH_2–O– in side chains), 3.05–4.76 (cellulose backbone; C$\underline{H}$ and $C\underline{H}_2$ in side chains). ^{13}C NMR (500 MHz, D_2O): 17.4–22.0 ($\underline{C}H_3$–CH(–OH)–CH_2–O– and (–O–CH(–$\underline{C}H_3$)–CH_2–)$_n$ in side chains), 28.3 ($\underline{C}H_3$–C(=O)–CH_2–O– in side chains), 68.2–107.0 (cellulose backbone; $\underline{C}$H and $\underline{C}H_2$ in side chains), 213.7 (CH_3–$\underline{C}$(=O)–CH_2–O– in side chains).

2.5. General procedure for synthesis of zwitterionic cellulose adducts

Ox-HPC (1 g, 2.3 mmol) was dissolved in 40 mL DI water in a round-bottom flask. ω-Aminoalkanoic acid (19.4 mmol, 4.7 equiv. per ketone group) was added to the solution with stirring, then sodium cyanoborohydride (2.44 g, 38.8 mmol, 9.3 equiv. per ketone group) was added to the solution. The solution was stirred at 37 °C for 48 h. After cooling to RT, the solution was dialyzed against DI water for 7 days, then finally freeze-dried to afford product.

2.6. Synthesis of HPC-glycine adduct (HPC-AA1)

Prepared according to the general procedure, with glycine (1.46 g, 19.4 mmol, 4.7 equiv. per ketone group) employed as the ω-aminoalkanoic acid. The product was a white fibrous material (1.07 g, yield 88%, DS(Zw) 1.6). ^{1}H NMR (500 MHz, D_2O): 1.15 ($C\underline{H}_3$–CH(–OH)–CH_2–O– and (–O–CH(–$C\underline{H}_3$)–CH_2–)$_n$ in side chains), 1.30 ($C\underline{H}_3$–CH(–N)–CH_2–O– in side chains), 3.05–4.76

(cellulose backbone; C<u>H</u> and C<u>H</u>$_2$ in side chains). ^{13}C NMR (500 MHz, D_2O): 15.6 (<u>C</u>H_3–CH(–N)–CH_2–O– in side chains), 17.4–22.0 (<u>C</u>H_3–CH(–OH)–CH_2–O– and (–O–CH(–<u>C</u>H_3)–CH_2–)$_n$ in side chains), 49.3 (–NH_2^+–<u>C</u>H_2–COO^- in side chains), 56.6 (CH_3–<u>C</u>H(–N)–CH_2–O– in side chains), 68.2–107.0 (cellulose backbone; CH_3–<u>C</u>H(–OH)–<u>C</u>H_2–O–, CH_3–CH(–N)–<u>C</u>H_2–O–, and (–O–<u>C</u>H(–CH_3)–<u>C</u>H_2–)$_n$ in side chains), 174.1 (–NH_2^+–CH_2–<u>C</u>OO^- in side chains).

2.7. Synthesis of HPC-(γ-aminobutyric acid) adduct (HPC-AA3)

Prepared according to the general procedure with γ-aminobutyric acid (2.00 g, 19.4 mmol, 4.7 equiv. to ketone groups) employed as the ω-aminoalkanoic acid. The product was a white fibrous material (1.11 g, yield 93%, DS(Zw) 1.0). ^{1}H NMR (500 MHz, D_2O): 1.15 (C<u>H</u>$_3$–CH(–OH)–CH_2–O– and (–O–CH(–C<u>H</u>$_3$)–CH_2–)$_n$ in side chains), 1.31 (C<u>H</u>$_3$–CH(–N)–CH_2–O– in side chains), 1.91 (–NH_2^+–CH_2–C<u>H</u>$_2$–CH_2–COO^- in side chains), 2.31 (–NH_2^+–CH_2–CH_2–C<u>H</u>$_2$–COO^- in side chains), 3.09 (–NH_2^+–C<u>H</u>$_2$–CH_2–CH_2–COO^- in side chains), 3.05–4.76 (cellulose backbone; CH_3–C<u>H</u>(–OH)–C<u>H</u>$_2$–O–, CH_3–C<u>H</u>(–N)–C<u>H</u>$_2$–O–, and (–O–C<u>H</u>(–CH_3)–C<u>H</u>$_2$–)$_n$ in side chains). ^{13}C NMR (500 MHz, D_2O): 15.6 (<u>C</u>H_3–CH(–N)–CH_2–O– in side chains), 17.4–22.0 (<u>C</u>H_3–CH(–OH)–CH_2–O– and (–O–CH(–<u>C</u>H_3)–CH_2–)$_n$ in side chains), 25.2 (–NH_2^+–CH_2–<u>C</u>H_2–CH_2–COO^- in side chains), 37.5 (–NH_2^+–CH_2–CH_2–<u>C</u>H_2–COO^- in side chains), 47.5 (–NH_2^+–<u>C</u>H_2–CH_2–CH_2–COO^- in side chains), 56.4 (CH_3–<u>C</u>H(–N)–CH_2–O– in side chains), 68.2–107.0 (cellulose backbone; CH_3–<u>C</u>H(–OH)–<u>C</u>H_2–O–, CH_3–CH(–N)–<u>C</u>H_2–O–, and (–O–<u>C</u>H(–CH_3)–<u>C</u>H_2–)$_n$ in side chains), 184.0 (–NH_2^+–CH_2–CH_2–<u>C</u>OO^- in side chains).

2.8. Synthesis of HPC-(5-aminovaleric acid) adduct (HPC-AA4)

Prepared according to the general procedure with 5-aminovaleric acid (2.28 g, 19.4 mmol, 4.7 equiv. to ketone groups) employed as the ω-aminoalkanoic acid. The product was a white fibrous material (1.11 g, yield 91%, DS(Zw) 0.9). ^{1}H NMR (500 MHz, D_2O): 1.15 (C<u>H</u>$_3$–CH(–OH)–CH_2–O– and (–O–CH(–C<u>H</u>$_3$)–CH_2–)$_n$ in side chains), 1.31 (C<u>H</u>$_3$–CH(–N)–CH_2–O– in side chains), 1.64 (–NH_2^+–CH_2–CH_2–C<u>H</u>$_2$–CH_2–COO^- in side chains), 1.68 (–NH_2^+–CH_2–C<u>H</u>$_2$–CH_2–CH_2–COO^- in side chains), 2.22 (–NH_2^+–CH_2–CH_2–CH_2–C<u>H</u>$_2$–COO^- in side chains), 3.08 (–NH_2^+–C<u>H</u>$_2$–CH_2–CH_2–CH_2–COO^- in side chains), 3.05–4.76 (cellulose backbone; CH_3–C<u>H</u>(–OH)–C<u>H</u>$_2$–O–, CH_3–C<u>H</u>(–N)–C<u>H</u>$_2$–O–, and (–O–C<u>H</u>(–CH_3)–C<u>H</u>$_2$–)$_n$ in side chains). ^{13}C NMR (500 MHz, D_2O): 15.6 (<u>C</u>H_3–CH(–N)–CH_2–O– in side chains), 17.4–22.0 (<u>C</u>H_3–CH(–OH)–CH_2–

O– and (–O–CH(–CH$_3$)–CH$_2$–)$_n$ in side chains), 25.5 (–NH$_2^+$–CH$_2$–CH$_2$–CH$_2$–CH$_2$–COO$^-$ in side chains), 28.3 (–NH$_2^+$–CH$_2$–CH$_2$–CH$_2$–CH$_2$–COO$^-$ in side chains), 39.6 (–NH$_2^+$–CH$_2$–CH$_2$–CH$_2$–CH$_2$–COO$^-$ in side chains), 47.2 (–NH$_2^+$–CH$_2$–CH$_2$–CH$_2$–CH$_2$–COO$^-$ in side chains), 56.4 (CH$_3$–CH(–N)–CH$_2$–O– in side chains), 68.2–107.0 (cellulose backbone; CH$_3$–CH(–OH)–CH$_2$–O–, CH$_3$–CH(–N)–CH$_2$–O–, and (–O–CH(–CH$_3$)–CH$_2$–)$_n$ in side chains) 185.5 (–NH$_2^+$–CH$_2$–CH$_2$–CH$_2$–CH$_2$–COO$^-$ in side chains).

2.9. Synthesis of HPC-(6-aminohexanoic acid) adduct (HPC-AA5)

Prepared according to the general procedure with 6-aminohexanoic acid (2.55 g, 19.4 mmol, 4.7 equiv. to ketone groups) employed as the ω-aminoalkanoic acid. The product was a white fibrous material (1.13 g, yield 89%, DS(Zw) 1.0). ^{1}H NMR (500 MHz, D$_2$O): 1.15 (CH$_3$–CH(–OH)–CH$_2$–O– and (–O–CH(–CH$_3$)–CH$_2$–)$_n$ in side chains), 1.31 (CH$_3$–CH(–N)–CH$_2$–O– in side chains), 1.38 (–NH$_2^+$–CH$_2$–CH$_2$–CH$_2$–CH$_2$–CH$_2$–COO$^-$ in side chains), 1.59 (–NH$_2^+$–CH$_2$–CH$_2$–CH$_2$–CH$_2$–CH$_2$–COO$^-$ in side chains), 1.70 (–NH$_2^+$–CH$_2$–CH$_2$–CH$_2$–CH$_2$–CH$_2$–COO$^-$ in side chains), 2.18 (–NH$_2^+$–CH$_2$–CH$_2$–CH$_2$–CH$_2$–CH$_2$–COO$^-$ in side chains), 3.07 (–NH$_2^+$–CH$_2$–CH$_2$–CH$_2$–CH$_2$–CH$_2$–COO$^-$ in side chains), 3.05–4.76 (cellulose backbone; CH$_3$–CH(–OH)–CH$_2$–O–, CH$_3$–CH(–N)–CH$_2$–O–, and (–O–CH(–CH$_3$)–CH$_2$–)$_n$ in side chains). ^{13}C NMR (500 MHz, D$_2$O): 15.7 (CH$_3$–CH(–N)–CH$_2$–O– in side chains), 17.4–22.0 (CH$_3$–CH(–OH)–CH$_2$–O– and (–O–CH(–CH$_3$)–CH$_2$–)$_n$ in side chains), 28.0 28.2 28.4 (–NH$_2^+$–CH$_2$–CH$_2$–CH$_2$–CH$_2$–CH$_2$–COO$^-$ in side chains), 40.0 (–NH$_2^+$–CH$_2$–CH$_2$–CH$_2$–CH$_2$–CH$_2$–COO$^-$ in side chains), 47.4 (–NH$_2^+$–CH$_2$–CH$_2$–CH$_2$–CH$_2$–CH$_2$–COO$^-$ in side chains), 56.3 (CH$_3$–CH(–N)–CH$_2$–O– in side chains), 68.2–107.0 (cellulose backbone; CH$_3$–CH(–OH)–CH$_2$–O–, CH$_3$–CH(–N)–CH$_2$–O–, and (–O–CH(–CH$_3$)–CH$_2$–)$_n$ in side chains), 186.0 (–NH$_2^+$–CH$_2$–CH$_2$–CH$_2$–CH$_2$–CH$_2$–COO$^-$ in side chains).

2.10. Titration

HPC-AA1 (60 mg) was dissolved in DI water (15 mL) in a 30 mL beaker with magnetic stirring. The pH meter was calibrated with a two-point calibration before starting the titration process. Solution pH was adjusted to 2 by adding 0.1 N HCl solution. Subsequently, the solution was titrated with 0.1 N NaOH until reaching pH of 12 under continuous stirring. The added base volume and solution pH at each point were recorded. Titration was performed in triplicate at RT.

2.11. Surface tension measurements

Surface tension values of polymer solutions prepared in 50 mM phosphate buffer (pH 6.8) at a polymer concentration of 50 μg/mL were determined using a KRÜSS Tensiometer (KRÜSS Scientific Instruments, Matthews, NC), which employs the Wilhelmy plate method to measure the surface tension of liquid samples. Each measurement was repeated at least 50 times with the goal of having a standard deviation less than or equal to 0.05 dyne/cm between the last 10 measurements.

2.12. Nucleation-induction time experiments

Polymers were dissolved in 15 mL 50 mM phosphate buffer (pH 6.8) at a concentration of 50 μg/mL and equilibrated for 60 min at 37 ºC. An enzalutamide supersaturated solution was created by adding a concentrated stock solution of the drug in MeOH to the polymer solution stirred at 300 rpm to yield a final drug concentration of 35 μg/mL. This is far above the reported crystalline solubility of 2.9 μg/mL, hence the solution is supersaturated (supersaturation ratio, which is the ratio of the observed solution concentration at supersaturation to that of the equilibrium solubility (that is to say, the thermodynamic solubility of the drug), is 35/2.9 = 12) (Wilson et al., 2020). The induction time, which is the time to detect the onset of crystallization in the solution, was measured using a SI Photonics UV-Vis spectrometer (Tucson, AZ) coupled to a fiber optic probe (path length 10 mm). The time at which there was an increase in scattering at a non-absorbing wavelength (380 nm) was recorded as the induction time. Experiments were performed in triplicate.

2.13. Determination of polymer-water Flory–Huggins interaction parameter

The isothermal water sorption and desorption profiles (**Figure S16**) were collected by placing polymer powders in a pan and exposing to increasing and then decreasing relative humidities (RH) using a Dynamic Vapor Sorption (DVS) Adventure System (Surface Measurement System, Allentown, PA). Each sample was equilibrated at 37 ºC and 0% RH for 60 min under a nitrogen purge, then the % RH was increased from 0 % to 95% with a 5 % increment step with an equilibrium criterion of < 0.005% change in 5 min. The relative vapor pressure obtained from the DVS data was used to calculate the Flory–Huggins interaction parameter using the following equation (Zhang & Zografi, 2000):

$$\ln (p/p_o) = \ln V_1 + (1- \frac{1}{x}) V_2 + \chi V_2^2 \quad (4)$$

where p is the partial pressure of water vapor, p_o is the saturation pressure of water at the designated temperature, V_1 is the volume fraction of the absorbed vapor, V_2 is the volume fraction of the polymer, x is the relative molecular volume of the polymer and χ is the Flory–Huggins interaction parameter. Calculations were based on HPC density (1.17 g/mL) (Samuels, 1969), with a molecular volume of 1.42E-19 cm^3/mol.

2.14. Preparation and dissolution of amorphous solid dispersion (ASD) films

ASD films containing 25 wt. % drug loading and either HPC or HPC-AA1 were prepared using a Buchi Rotavapor-R (Newcastle, Delaware) equipped with Yamato BM-200 water bath set at 70 °C. In brief, enzalutamide and the polymer were dissolved in methanol in a scintillation vial followed by drying to form a film, which upon complete dissolution would generate solutions with a supersaturation level of either 12 or 6.8. The films were prepared in scintillation vials and left overnight under vacuum to ensure complete solvent removal. All dissolution studies were conducted in triplicate in 50 mM phosphate buffer (pH 6.8) using a Hanson Vision G2 Classic 6 dissolution system (Teledyne Hanson Research, Chatsworth, CA), and an *in situ* Rainbow fiber optic ultraviolet spectrometer coupled with 10 mm fiber optic dip probes (Pion, Billerica, MA, USA) was used to monitor drug concentration over time. Second derivative analysis was applied to correct the spectral baseline and the area under the curve was determined over the spectral range of 310 – 320 nm. A calibration curve for enzalutamide was built over a concentration range 1 – 70 μg/mL.

3. Results and discussion

In this work, a highly substituted commercial HPC was chosen as starting material. We hypothesized that by chemoselectively oxidizing the terminal secondary hydroxy groups of the oligo(hydroxypropyl) substituents to ketones, using simple household bleach and a modification of our recently published method (Nichols et al., 2020), we would create an ideal substrate for adding ω-aminoalkanoic acid substituents by reductive amination. In the event, bleach oxidation of the HPC terminal secondary hydroxy groups afforded DS(ketone) of Ox-HPC up to 1.8, creating ample amine-reactive groups. Reductive amination is one of the most important methods for C–N

single bond construction, and involves nucleophilic attack of an amine upon (in our case) the ketone with loss of water to form imine bonds (Silva, 2020; Zhou, Petrova, & Edgar, 2021). The imine is then reduced to an amine, often using a borohydride derivative (Zhang & Edgar, 2015); this can be carried out in a separate step, or *in situ* to create a one-pot process from ketone to amine. Tertiary amines have frequently been used to introduce zwitterionic moieties in post-polymerization processes; it can be anticipated that the primary amines of ω-aminoalkanoic acids would be much better nucleophiles, leading to higher, faster conversions (Kanzian, Nigst, Maier, Pichl, & Mayr, 2009; Zhou & Edgar, 2022).

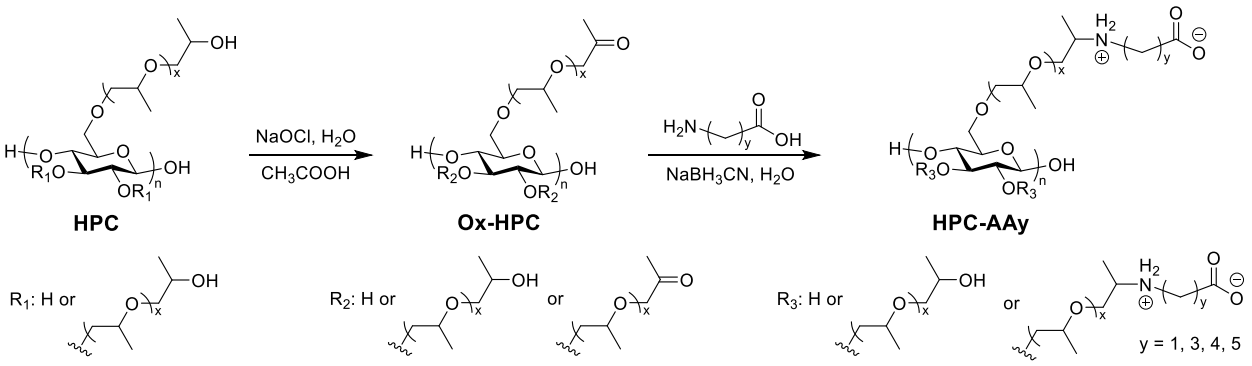

Scheme 1. Two-step synthesis of zwitterionic cellulose adducts starting from HPC. Products are referred to herein as HPC-AA1, HPC-AA3, HPC-AA4, and HPC-AA5, corresponding to y = 1, 3, 4, and 5 respectively in the scheme above. Note that structures in this and other figures are not meant to imply regioselective substitution; depictions used are merely for clarity and simplicity for the reader.

3.1. Synthesis and characterization of zwitterionic cellulose adducts

Water was chosen as a green, benign, inexpensive solvent for reductive amination of HPC, and we chose to explore the potentially efficient one-pot approach. The equilibrium between non-zwitterionic and zwitterionic forms of ω-aminoalkanoic acids in aqueous solution was taken advantage to facilitate the reactions (Kaßner, Kronawitt, Klimm, Seifert, & Spange, 2019). Moderate temperatures (37°C) were explored for the condensation between Ox-HPC ketones and the amine termini of the ω-aminoalkanoic acids, based on our previous work preparing all-

polysaccharide hydrogels by reaction of Ox-HPC ketones with the amino groups of chitosan (Chen et al., 2020; Zhou, Zhai, et al., 2022). These reductive aminations could be monitored by ^{1}H NMR spectroscopy, and product structures were confirmed by FTIR, as well as by ^{1}H NMR, ^{13}C, ^{1}H–^{1}H COSY, and ^{1}H–^{13}C HSQC NMR spectroscopic methods. **Figure 1** shows an overlay of the ^{1}H NMR spectra of Ox-HPC and its zwitterionic derivatives. The methyl group of Ox-HPC adjacent to the new ketone resonates at 2.2 ppm. After reductive amination with glycine, that methyl resonance almost completely disappeared. A new resonance appeared at 1.3 ppm, which we assigned to the methyl groups adjacent to the secondary amine (a" in the spectrum of HPC-AA1, **Figure 1**).

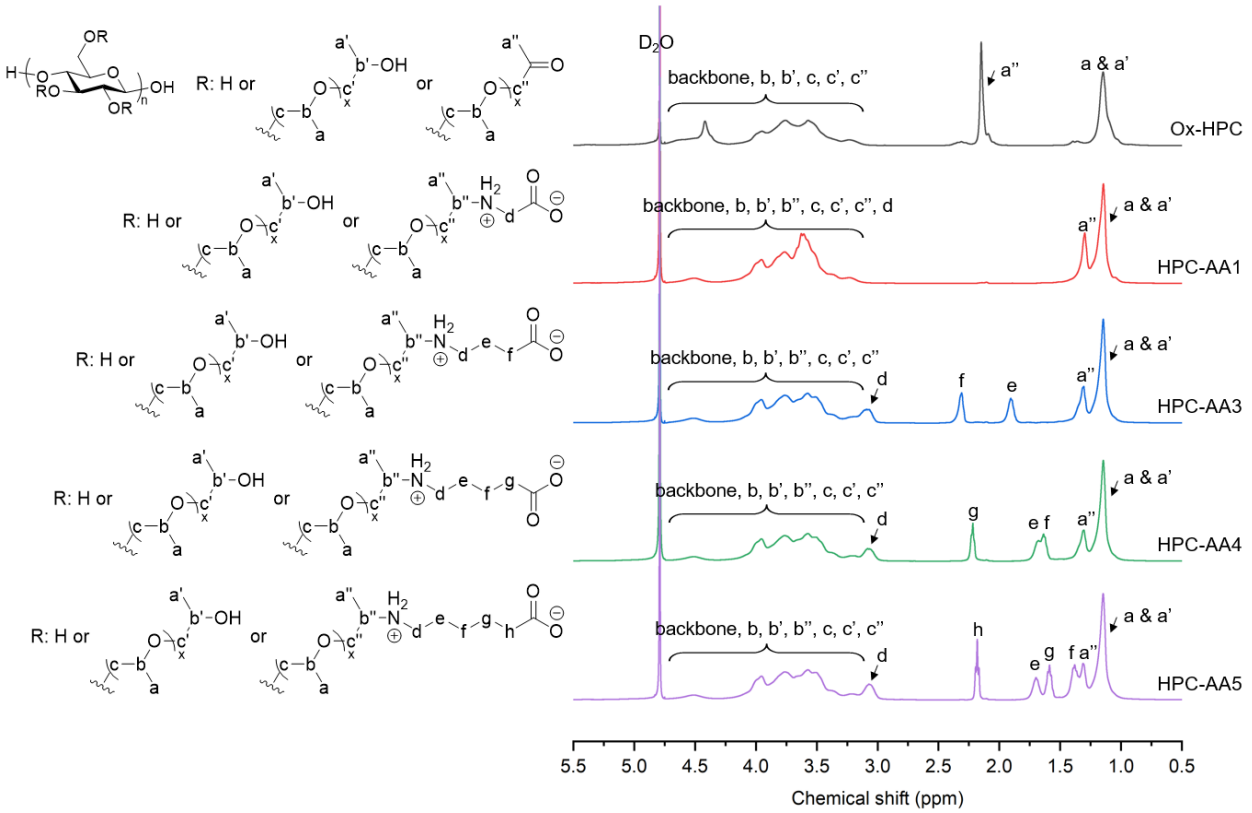

Figure 1. ^{1}H NMR spectra of Ox-HPC, HPC-AA1, HPC-AA3, HPC-AA4, and HPC-AA5.

The DS(Zw) of product HPC-AA1 was 1.6, calculated from the ratio of integrals of resonances a" and (a & a'), corresponding to 91% of the available ketone groups having been reductively aminated. The high DS(Zw) achieved can be attributed to the structure of Ox-HPC and ω-aminocarboxylic acids, where the Ox-HPC ketones at the termini of the oligo(HP) substituents

have broader approach angles compared to the functionalities on the polysaccharide backbone (Zhou et al., 2021), and the glycine amines likewise have wide approach angles. We selected sodium cyanoborohydride for the reduction step, since it is a less reactive, more selective reducing agent for reductive amination (Clinton, 1975). However, competitive direct reduction of the ketones to hydroxyls was still a concern as a potential side-reaction (Borch, Bernstein, & Durst, 1971; Clinton, 1975). It was possible to quantify the direct ketone reduction side reaction by difference; subtracting the measured values (^{1}H NMR) of DS(Zw) from the original DS(ketone), and subtracting the measured residual ketone from that number, afforded an estimate of the amount of ketone reduction. In the reductive amination of Ox-HPC with glycine, ca. 9% of the original ketone groups were lost due to the side reaction of reduction to hydroxy groups.

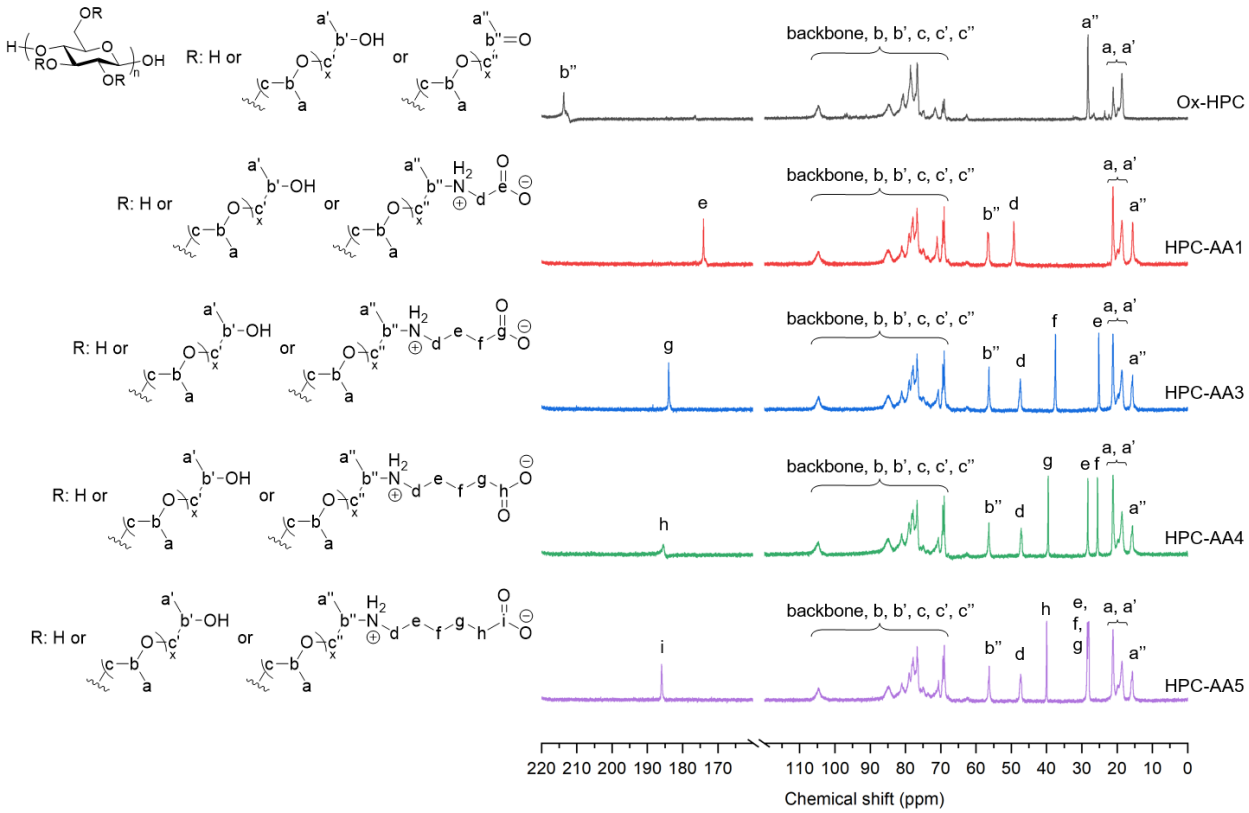

Figure 2. ^{13}C NMR spectra of Ox-HPC, HPC-AA1, HPC-AA3, HPC-AA4, and HPC-AA5.

Further characterization evidence was provided by the HPC-AA ^{13}C NMR spectra **(Figure 2)**, where the resonance of the methyl next to the ketone group at 28 ppm in Ox-HPC moved to 16 ppm in HPC-AA1 after reductive amination, supporting the expected formation of the new

secondary amine. The ^{13}C resonance at 16 ppm was correlated to the proton at 1.3 ppm in the ^{1}H–^{13}C HSQC spectrum, supporting this assignment **(Figure S2)**. A new resonance attributed to the methylene of the glycine substituent was observed at 49 ppm. It was correlated in HSQC with a proton at roughly 3.6 ppm, within the backbone region of cellulose, consistent with the expected shift of the glycine methylene. Ketone carbons resonated at 214 ppm in the ^{13}C NMR spectrum of Ox-HPC, but in the ^{13}C spectrum of HPC-AA1 the ketone resonance was not significant, consistent with high conversion of ketone to imine (and a much lower percentage of alcohol). On the other hand, a resonance assigned to the glycine carboxyl group at 174 ppm was observed in HPC-AA1. No ^{13}C resonance was observed at 44 ppm, which is the chemical shift of the glycine alpha-carbon, indicating that there was no significant evidence for free glycine in the product.

It was of interest to investigate the influence of the length of the oligo(methylene) linker between amine and carboxyl upon reactivity, product solubility, and other properties, and ultimately upon performance in ASD and other applications. Therefore, we sought to broaden the applicability of this reductive amination approach to include 4-aminobutyric acid (γ-aminobutyric acid, or GABA; an important neurotransmitter (Michels et al., 2012)), 5-aminovaleric acid, and 6-aminohexanoic acid as potential reactants. These condensations were also all attempted in water, at 37 °C, and for 48 h. The signature resonance for methyl groups at the oligo(HP) chain termini, next to the appended amine substituent, was observed at ca. 1.3 ppm in each product ^{1}H NMR spectrum. In each case, the proton resonance for the methyl group adjacent to the ketone in Ox-HPC at 2.2 ppm was insignificant, illustrating near complete consumption of ketone after 48 h. Conversions for products with tethers longer than that of glycine were easier to calculate because they possessed at least one methylene that was not proximal to a strong electron-withdrawing group (thus not overlapping with the cellulose backbone region or other resonances) that could be observed and quantified from the ^{1}H NMR spectrum. Conversion of ketone moieties to zwitterionic ω-aminoalkanoate substituents was somewhat lower overall for ω-aminoalkanoates with longer oligo(methylene) tethers, with DS(Zw) decreasing from 1.6 for glycine to between 0.9 – 1.0 for the higher analogs, as determined by ^{1}H NMR integration ratios **(Table 1)**. In the ^{13}C NMR spectra of these products, no significant ketone carbon was observed, consistent with near-complete conversion of the ketone. In each case a new resonance at 16 ppm was present, assigned to the methyl group near the new formed secondary amine. All expected carbon and proton resonances from the internal methylenes of the appended ω-aminoalkanoate substituents were

present as expected and with predictable chemical shifts, supporting successful synthesis of the targeted reductive amination products. It is also noteworthy that these chemical shifts of methylenes adjacent to amine all differed from those of the corresponding groups in the monomeric ω-aminoalkanoate reactants **(Figure S9)**; there was no evidence of monomeric contaminants in the products. Resonance assignments for the appended ω-aminoalkanoate moieties were supported by $^{1}H–^{1}H$ COSY and $^{1}H–^{13}C$ HSQC NMR spectra **(Figure S3 – S8)**. All the methylenes in ω-aminocarboxylic acids could be identified even more easily by $^{1}H–^{13}C$ HSQC NMR spectra because they appeared as blue in the negative phase. Proton resonances at 3.1 ppm were particularly distinctive and were assigned to the methylene adjacent to the newly formed secondary amine. The proton spectra also revealed, by the difference methods (DS(ketone) – DS(Zw)) described above, that the lower conversion of ketones to ω-aminoalkanoate substituents for the ω-aminoalkanoates with tethers longer than that of glycine was due to competing direct reduction of the ketone by sodium cyanoborohydride, where about 40% of the ketone groups were reduced to secondary hydroxy groups. We speculate that this was due to slower kinetics for condensation of the higher ω-aminoalkanoates with Ox-HPC ketones. This is surely influenced by steric factors, but could also be influenced by self-association of the higher ω-aminoalkanoate analogs in water, due to their larger proportions of hydrophobic components.

Table 1. Conversions to zwitterionic polysaccharides and DS(Zw).

	HPC-AA1	HPC-AA3	HPC-AA4	HPC-AA5
Conversion	91%	54%	52%	57%
DS	1.6	1.0	0.9	1.0

3.2. Polymer properties

FTIR spectra were recorded to gather further evidence for product identities **(Figure 3)**. Broad absorbances near 3440 cm^{-1} corresponding to O−H stretching vibrations, at 2965 cm^{-1} and 2870 cm^{-1} corresponding to C−H stretching vibrations, and at 1056 cm^{-1} (C−O−C stretching vibration) were observed for all cellulose derivatives. Ox-HPC displayed the expected C═O ketone

stretch at 1712 cm^{-1} (Eguchi, Kawabata, & Goto, 2017; Nichols et al., 2020; Zhang et al., 2016).

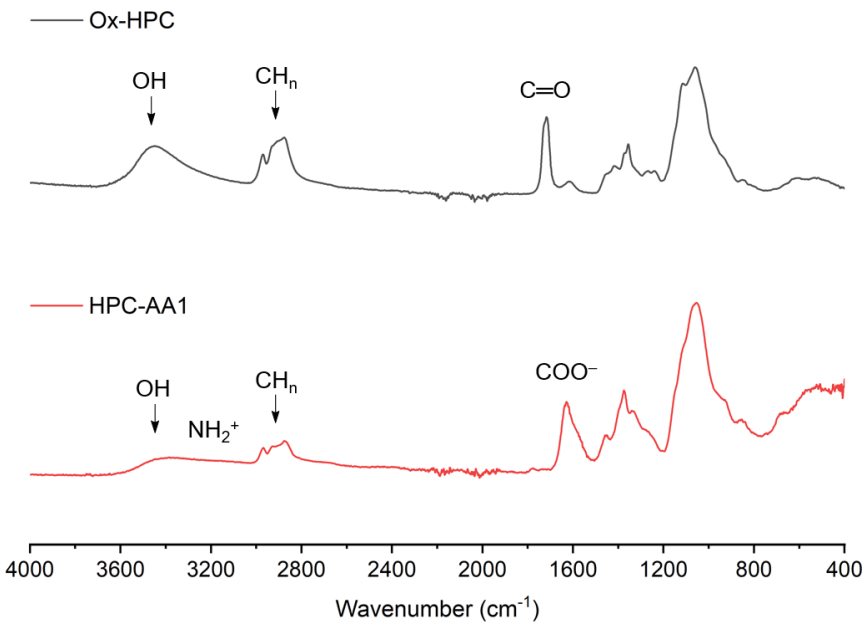

Figure 3. FTIR spectra of Ox-HPC, and HPC-AA1.

No significant ketone stretch (ca. 1700 cm^{-1}, see Ox-HPC spectrum, **Figure 3**) was observed in reductive amination product spectra. The key features supporting the purported reductive amination product structures were the broad absorbances in the vicinity of 3200 cm^{-1}, attributed to N−H stretch, and the moderately strong absorbances centered at approximately 1620 cm^{-1}, attributed to the ionized carboxylates (COO^-). In the FTIR spectrum of HPC-AA1, a broad band between O−H stretch and C−H stretch appeared, likely resulting from N−H stretching vibrations. The band at 1624 cm^{-1} can be attributed to COO^- asymmetric stretching. These assignments reference (Ambujam, Selvakumar, Prem Anand, Mohamed, & Sagayaraj, 2006; Kumar, Vizhi, Sivakumar, Vijayan, & Babu, 2012; Mary, Ushakumari, Harikumar, Varghese, & Panicker, 2009; Rosado, Duarte, & Fausto, 1998). Regarding the FTIR spectra of HPC-AA3, HPC-AA4, and HPC-AA5 **(Figure S10)**, absorbances at around 1560 cm^{-1} were observed. These characteristic absorbances could be attributed to COO^- asymmetric stretching (Vamecq et al., 2009). A weak peak of N−H bending might be overlapped between 1620 − 1560 cm^{-1} (Heacock & Marion, 1956; Smith, 2019; Smith, 2018).

^1H NMR spectra (**Figure S11**) confirmed that the amines of the polymers were in

protonated form in aqueous solution. We compared the ^{1}H NMR spectra of HPC-AA3 in D_2O, and 10 vol% acetic acid-d_4 in D_2O. The protons a'' and d near the amine did not change chemical shifts significantly upon addition of acetic acid. This evidence supports the hypothesis that the amines are in protonated form in D_2O or water, as expected if the polymer is zwitterionic. Based on this evidence and on supportive facts and theory (the pKa values of amines (ca. 10) and carboxylic acids (ca. 4.5), and the fact that natural amino acids are zwitterionic at neutral pH), we are confident that the ω-aminocarboxylic acid reductive amination products (HPC-AA) are in zwitterionic form in neutral or near-neutral aqueous solutions.

A titration experiment was conducted to determine the effect of pH on product ionization state (**Figure 4**). An HPC-AA1 solution was acidified and subsequently titrated with base from pH 2 to 12. The titration profile showed a similar trend compared to that of glycine (Darvey & Ralston, 1993). The two distinct inflection points indicated the deprotonation of carboxylic acid and secondary ammonium ion, respectively. HPC-AA1 was primarily in its zwitterionic form in the pH range between 4 – 8. It implies that as an oral drug carrier, the adducts would be mostly in zwitterionic form in the environments of most important sites of oral drug absorption: small intestine (pH range of 6.6 – 7.5) and colon (pH range of 6.4 – 7.0) (Evans et al., 1988). Under strong acidic or alkaline conditions, HPC-AA1 showed a net positive or negative charge.

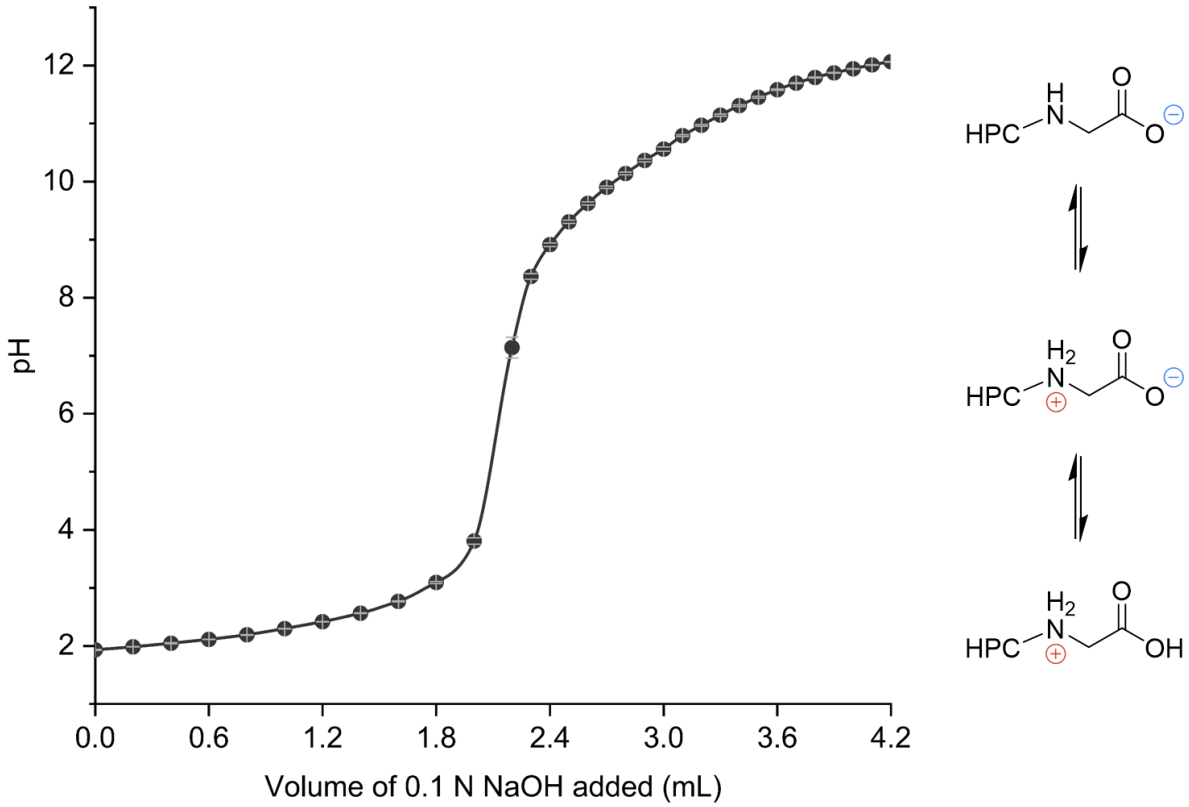

Figure 4. Titration profile of HPC-AA1.

Given the potential impact on polymer thermal stability of the introduced charged groups, structure-property relationships were further probed by TGA. Preliminary TGA experiments revealed that the zwitterionic products were hygroscopic, which was unsurprising given the abundance of charged groups. Therefore, all samples were dried at 80 °C overnight under vacuum prior to TGA analysis in order to remove free water, and potentially some bound water. Less than 1 wt% weight loss occurred up to 150 °C. According to the TGA (**Figure S12**) and (Derivative Thermogravimetry) DTG (**Figure S13 − S14**) curves of the products, significant weight loss of all samples began at ca. 200 °C, indicating the start of pyrolysis (Zhang et al., 2021). The majority of the weight loss occurred between 250 – 400 °C. The fastest weight loss HPC-AA1 was at ca. 300 °C, which was lower than that for Ox-HPC (ca. 330 °C). This phenomenon is consistent with previous studies indicating that the introduction of zwitterionic side chains is not conducive for the thermal stability of the polymer (Ma, Zhou, Wu, & Zhang, 2011). Meanwhile, HPC-AA3,

HPC-AA4, and HPC-AA5 exhibited the fastest weight loss temperature at ca. 350 °C. Factors including lower DS(Zw) and extended side chains possibly led to an increased resistance to degradation (Heinze, Mang, Popescu, & Weichold, 2016). The 5% weight loss temperature (T_{d5}) is frequently used to characterize polymer thermal stability. HPC-AA3, HPC-AA4, and HPC-AA5 showed slightly higher T_{d5} values than Ox-HPC, while HPC-AA1 had the lowest T_{d5} (214 °C). This observation may have been due to the higher DS(Zw) of HPC-AA1 and higher hydrophilicity of glycine compared to other ω-aminocarboxylic acids. Overall, the zwitterionic cellulose derivatives were relatively thermally stable.

Glass transition temperature (T_g) is an important property of amorphous polymers for many applications, reflecting macro-manifestation of chain flexibility (Wang, Zheng, & Zheng, 2011). With regard to potential application in ASD, T_g has particular importance; ASDs are metastable molecular dispersions of amorphous bioactive compounds in polymer matrices. For storage stability, it is critical that ASD formulations have T_g values above ambient temperature (i.e., remain in the glassy phase) even at high ambient temperatures, in high humidity, and when the bioactive species happens to be a plasticizer for the polymer. T_g values obtained from DSC are shown in **Table 2**. Further analysis of the DSC results reveals that ω-aminoalkanoate-substituted, zwitterionic derivatives did not exhibit crystallization or melting thermal transitions, supporting the contention that all derivatives were amorphous. All zwitterionic products displayed T_g values higher than that of the starting polymer Ox-HPC (T_g 81 °C). The zwitterionic side chains are capable of strong dipole−dipole interactions which may restrict polymer flexibility (Bengani-Lutz, Converse, Cebe, & Asatekin, 2017); T_g of HPC-AA1 reached 135 °C with its high DS(Zw). As the oligo(methylene) tether length increased, and with lower DS(Zw), the higher analogs displayed lower T_g values than that of the glycine adduct (but still higher than Ox-HPC).

Table 2. Thermal properties of zwitterionic cellulose derivatives: glass transition (T_g) and 5% weight loss (T_{d5}) temperatures.

	T_g (°C)	T_{d5} (°C)
Ox-HPC	81	242
HPC-AA1	135	214

HPC-AA3	92	247
HPC-AA4	96	246
HPC-AA5	94	247

Water solubility is a key property for many applications, not least for ASD. ASD polymers must have sufficient aqueous solubility to release the drug in the aqueous medium of the gastrointestinal (GI) tract, and it is beneficial that the polymer dissolve rapidly, since this controls the drug release rate (Saboo, Mugheirbi, Zemlyanov, Kestur, & Taylor, 2019). Solubility of the HPC ω-aminoalkanoate reductive amination products was evaluated **(Table 3)** in water, dimethyl sulfoxide (DMSO), *N*,*N*-dimethylacetamide (DMAc), methanol, ethanol, and acetone (the last three being important solvents for spray-drying of ASD formulations). All ω-aminoalkanoate products were soluble in water because of their high ionic content. Polar organic solubility of the derivatives was influenced by the length of the oligo(methylene) tether. Products HPC-AA1 and HPC-AA3 were soluble in methanol, but HPC-AA4 and HPC-AA5 were not. No products were soluble in the less polar solvents ethanol and acetone.

Table 3. Solubility of zwitterionic polymers.

	Ox-HPC	HPC-AA1	HPC-AA3	HPC-AA4	HPC-AA5
Water	+	+	+	+	+
DMSO	+	S	+	S	+
DMAc	+	–	–	S	S
Methanol	+	+	+	S	S
Ethanol	S	–	–	–	–
Acetone	–	–	–	–	–

(+) soluble; (–) insoluble; (S) swellable.

Conditions: Visual examination using 5 mg sample in 1 mL solvent after vortex mixing for 5 min, followed by gentle rolling overnight. Solubility of Ox-HPC was from (Zhou, Zhai, et al., 2022).

HPC is a thermoresponsive polymer that displays a lower critical solution temperature (LCST) in aqueous solution (usually between 40 and 45 °C), as do several cellulose ethers (Gosecki, Setälä, Virtanen, & Ryan, 2021; Weißenborn & Braunschweig, 2019). The mechanism of thermal gelation by cellulose ethers is still the subject of active investigation. Generally it is accepted that cellulose ethers like HPC interact strongly with water at lower temperatures (e.g. room temperature), but the hydrophobic interaction between polymer chains lead to coil-to-globule transition at temperatures above their LCST and, frequently, gelation (Coughlin et al., 2021; Pasparakis & Tsitsilianis, 2020). We measured the lowest temperature at which visible phase transition of HPC, Ox-HPC, and the zwitterionic adducts could be observed **(Table 4)**. Solutions of Ox-HPC started to become turbid at 64 °C, even though Ox-HPC has significantly fewer hydroxyl groups than HPC. No turbidity of the zwitterionic adduct solutions was observed up to 99 °C. It is likely that the stronger interaction between the zwitterionic sidechains and water is more persistent even at higher temperatures.

Table 4. Thermoresponsivity of zwitterionic polymers.

	HPC	Ox-HPC	HPC-AA1	HPC-AA3	HPC-AA4	HPC-AA5
Phase transition [a]	37 °C	64 °C	None [b]	None [b]	None [b]	None [b]

Measurements at 100 mg polymer/1 mL water.

[a] Lowest temperature of visible phase transition.

[b] No turbidity observed up to 99 °C.

3.3. Application of the zwitterionic cellulose adducts as ASDs

Besides high T_g, the hydrophilic/hydrophobic balance of polymers is also considered as a key factor for inhibiting drug crystallization effectively because the polymer must interact with the

hydrophobic drug, both in the solid pill and in the aqueous medium of the GI tract (Dong, Mosquera-Giraldo, Taylor, & Edgar, 2016). However, if the polymer becomes too hydrophobic, self-interactions are favored over interactions with the drug, hence, a fine balance is required (Mosquera-Giraldo et al., 2016). The zwitterionic cellulose adducts have high aqueous solubility; this could assist rapid drug release from the ASD, but could impede the necessary association with the hydrophobic drug. We evaluated the ability of these polymers to inhibit crystallization using the hydrophobic, poorly soluble (< 3 μg/mL), fast-crystallizing, anti-prostate cancer drug enzalutamide as a challenging model drug, by *in vitro* experiments.

The induction time measurements (**Figure 5**) show that the zwitterionic polymers were more effective as crystallization inhibitors than precursor HPC. These polymers may have a better amphiphilic balance, because of the hydrophilic zwitterionic groups and hydrophobic hydrocarbon portions of the side chains, allowing them to have more favorable interactions with both the hydrophobic drug and the aqueous solution (Mosquera-Giraldo et al., 2016). It has been shown that the conformation of the commercial polymer, hydroxypropyl methyl cellulose (hypromellose) acetate succinate at the solid-liquid interface of the hydrophobic drug surface depends on the polymer's ionization state (Schram et al., 2015). Higher degrees of ionization caused the polymer chains to repel one another with reduced tendency to form coiled globules, allowing for more uniform adsorption on the crystal surface and thereby more efficient maintenance of the supersaturated state. Zwitterionic polymers may have an added advantage as they remain ionized over a wide pH range, allowing for maintenance of supersaturation across a larger absorption window throughout the GI tract. It is notable that all HPC-AA polymers increased crystallization induction time at least to > 150 min, even in an *in vitro* test where enzalutamide permeation through the epithelial membrane was not possible. In the actual small intestine where permeation occurs as well as dissolution, 2.5 h may be more than enough delay in crystallization to greatly enhance bioavailability, even for the extremely challenging drug enzalutamide.

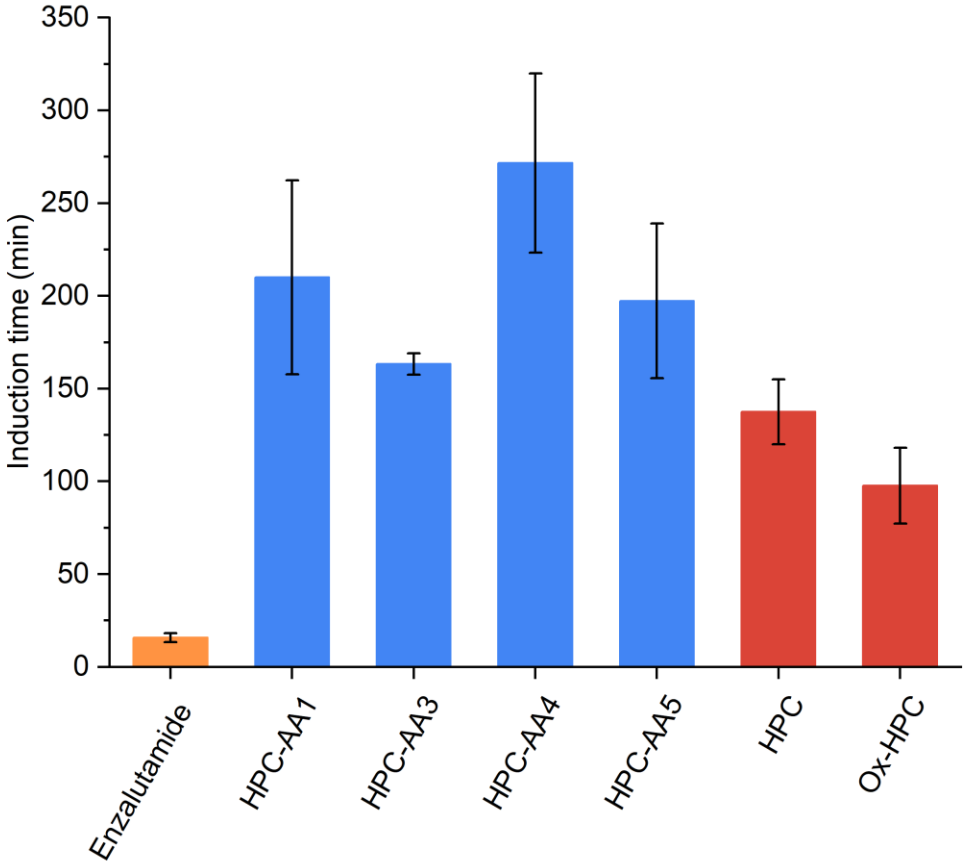

Figure 5. Mean induction time measurements of supersaturated enzalutamide solutions (35 µg/mL) in presence of 50 µg/mL pre-dissolved polymer. Error bars represent standard deviations, n = 3.

The amphiphilicity of the polymers is reflected in the surface tension measurements (**Table 5)** where it can be noted that all HPC-AA polymers have similar ability to reduce the surface tension of water as does the starting material, HPC. While the surface tension measurements do not trend exactly with the induction time measurements discussed above, they provide an indication of the tendency of the polymers to adsorb at a hydrophobic (air)-hydrophilic interface, and provides surrogate information about adsorption tendency at the crystal-water interface. Amphiphilic polymers are known to adsorb on the crystal-water interface, blocking access of solute molecules to the crystal surface, and decreasing the rate of crystallization (Schram, Taylor, & Beaudoin, 2015). However, while adsorption is a prerequisite for preventing incorporation of molecules into the crystal lattice, the conformation of the adsorbed polymer is also important

(Schram, Beaudoin, & Taylor, 2015; Schram, Taylor, et al., 2015); this is determined by interactions with both the solid surface and the aqueous media. The importance of the polymer conformation at the crystal-water interface may well explain the lack of direct correlation between polymer surface tension measurements and induction times. The Flory–Huggins interaction parameters shown in **Table 5** provide a measure of how favorable the interaction is with water, whereby lower values indicate better interactions. Based on these values, zwitterionic polymers interact more favorably with water compared to HPC, and as a result, may have more extended conformations on the crystal surface. This extended conformation, in turn, may provide more efficient blocking of crystal growth (Schram, Beaudoin, et al., 2015).

Table 5. Aqueous-air surface tension (pH 6.8) and Flory–Huggins interaction parameters of zwitterionic polymers at a polymer concentration of 50 µg/mL [a].

	HPC	Ox-HPC	HPC-AA1	HPC-AA3	HPC-AA4	HPC-AA5
Surface tension (dyne/cm)	43.63 (0.05)	49.66 (0.05)	43.63 (0.05)	47.43 (0.05)	52.36 (0.05)	43.11 (0.05)
Flory–Huggins interaction parameter (χ)	2.18	ND [b]	1.63	1.24	1.33	1.43

[a] Standard deviations are shown in parentheses, where n = 20.

[b] ND: Not determined.

These differences are reflected in the release data for amorphous solid dispersion films made with enzalutamide and either HPC-AA1 or HPC. Both polymers enabled rapid and complete release of the drug as they are both water-soluble, however at the higher supersaturation ratio, the HPC-AA1 polymer was able to maintain the supersaturated concentration without crystallization for 200 mins compared to 120 mins in the case of HPC, as shown in **(Figure 6a).** A longer duration, higher supersaturation ratio is favorable to promote drug absorption as the dosage form transits through the small intestine. Both polymers maintained supersaturation for 6 h at a lower supersaturation ratio as shown in **(Figure 6b).**

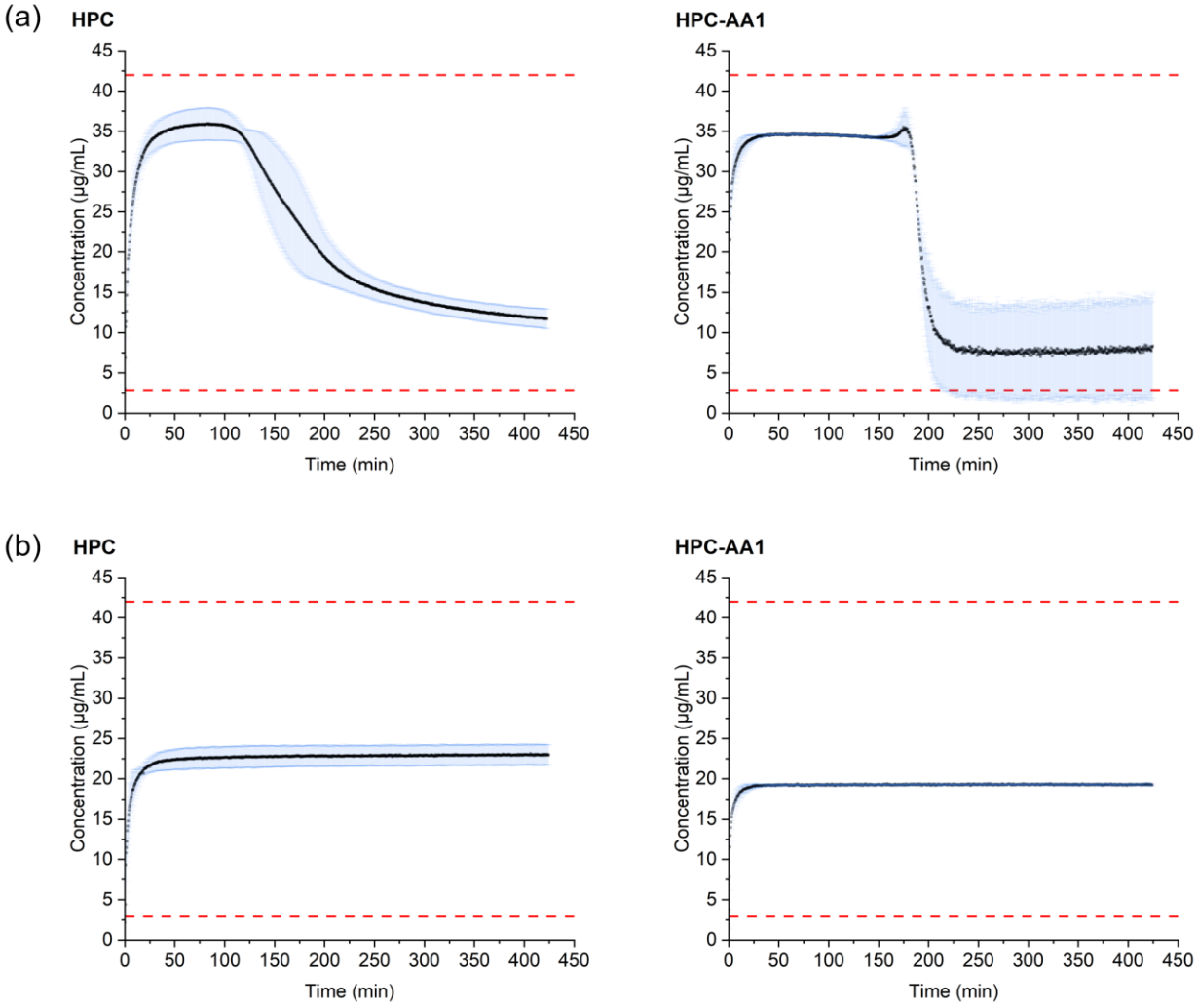

Figure 6. Dissolution profiles of HPC and HPC-AA1 ASD films at two different supersaturation ratios: (a) 12 and (b) 6.8. The upper and lower dashed lines represent the amorphous and crystalline solubility of enzalutamide as previously determined (Wilson et al., 2018). Error bars represent standard deviations, n = 3.

4. Conclusions

We have successfully demonstrated a new approach to zwitterionic cellulose derivatives by exploiting reductive amination of selectively oxidized hydroxypropyl cellulose and readily

611 available ω-aminocarboxylic acids. The ω-aminoalkanoate-substituted products exhibited
612 interesting properties including excellent thermal stability, tailorable solubility, and highly
613 effective crystallization inhibition of the hydrophobic, fast-crystallizing, anti-cancer drug
614 enzalutamide. The ability to make zwitterionic polymers with high DS(Zw) is a valuable and
615 unusual feature of this method. Overall, this work provides a simple, efficient, versatile, cost-
616 effective synthetic strategy for preparing zwitterionic cellulose derivatives of readily adjustable
617 properties, providing promise for pharmaceutical and other applications. Clearly it should be
618 applicable to any natural polysaccharide, since all polysaccharides possess hydroxy groups that
619 can be reacted with propylene oxide to append oligo(hydroxypropyl) groups that can then be
620 oxidized and reductively aminated; it is reasonable to anticipate that hydroxypropylation of amine
621 groups (e.g. of 2-amino-2-deoxy groups on polysaccharides such as chitosan) could also be a
622 useful entrée to such derivatives. The ability of these zwitterionic polymers to dissolve in water
623 offers great promise for their application from aqueous-based coating systems; this ability could
624 enable green surface coatings (with solubility adjustable by post-application crosslinking) with
625 antibacterial, antifouling, or other useful properties.

626

627 **CRediT authorship contribution statement**

628 Yang Zhou: Conceptualization, Methodology, Investigation, Validation, Formal analysis,
629 Visualization, Writing – original draft, Writing – review & editing.

630 Yimin Yao: Investigation, Validation, Formal analysis, Writing – review & editing.

631 Zhenghao Zhai: Investigation, Validation, Writing – review & editing.

Mennatallah A. Mohamed: Investigation, Formal analysis, Visualization, Writing – original draft.

Fiorella Mazzini: Investigation, Formal analysis.

Qingqing Qi: Investigation, Formal analysis.

Michael J. Bortner: Methodology, Formal analysis, Writing – review & editing, Resources.

Lynne S. Taylor: Methodology, Formal analysis, Writing – review & editing, Resources.

Kevin J. Edgar: Conceptualization, Methodology, Formal analysis, Writing – review & editing, Resources, Supervision.

Declaration of competing interest

The authors declare that they have no conflict of interest.

Acknowledgements

We thank the Virginia Tech Institute for Critical Technology and Applied Science, the Department of Sustainable Biomaterials, and the College of Natural Resources and Environment for partial support of this work. We are grateful for the David W. Francis & Lillian Francis Research Fellowship (YZ) which provided partial support of this work. We are grateful to the U.S. Department of Agriculture (NIFA) for partial support of this work through grant 2020-67021-31379 (ZZ). We thank the U.S. National Science Foundation for partial support of this

work through grants DMR-2204996 and DMR-2204995 (MM, QQ). We thank Dr. Murthy Shanaiah for guidance about NMR experiments.

References

Ambujam, K., Selvakumar, S., Prem Anand, D., Mohamed, G., & Sagayaraj, P. (2006). Crystal growth, optical, mechanical and electrical properties of organic NLO material γ-glycine. *Crystal Research and Technology: Journal of Experimental and Industrial Crystallography,* 41(7), 671-677.

Amer, H., Nypelö, T., Sulaeva, I., Bacher, M., Henniges, U., Potthast, A., & Rosenau, T. (2016). Synthesis and characterization of periodate-oxidized polysaccharides: dialdehyde xylan (DAX). *Biomacromolecules,* 17(9), 2972-2980.

Arca, H. C., Mosquera-Giraldo, L. I., Bi, V., Xu, D., Taylor, L. S., & Edgar, K. J. (2018). Pharmaceutical applications of cellulose ethers and cellulose ether esters. *Biomacromolecules,* 19(7), 2351-2376.

Arca, H. C., Mosquera-Giraldo, L. I., Taylor, L. S., & Edgar, K. J. (2017). Synthesis and characterization of alkyl cellulose ω-carboxyesters for amorphous solid dispersion. *Cellulose,* 24(2), 609-625.

Bengani-Lutz, P., Converse, E., Cebe, P., & Asatekin, A. (2017). Self-assembling zwitterionic copolymers as membrane selective layers with excellent fouling resistance: effect of zwitterion chemistry. *ACS applied materials & interfaces,* 9(24), 20859-20872.

Blackman, L. D., Gunatillake, P. A., Cass, P., & Locock, K. E. (2019). An introduction to zwitterionic polymer behavior and applications in solution and at surfaces. *Chemical Society Reviews,* 48(3), 757-770.

Borch, R. F., Bernstein, M. D., & Durst, H. D. (1971). Cyanohydridoborate anion as a selective reducing agent. *Journal of the American Chemical Society,* 93(12), 2897-2904.

Calabrese, V., da Silva, M. A., Schmitt, J., Muñoz-Garcia, J. C., Gabrielli, V., Scott, J. L., Angulo, J., Khimyak, Y. Z., & Edler, K. J. (2018). Surfactant controlled zwitterionic cellulose nanofibril dispersions. *Soft Matter,* 14(38), 7793-7800.

Chen, J., Nichols, B. L., Norris, A. M., Frazier, C. E., & Edgar, K. J. (2020). All-polysaccharide, self-healing injectable hydrogels based on chitosan and oxidized hydroxypropyl polysaccharides. *Biomacromolecules,* 21(10), 4261-4272.

Cheng, G., Li, G., Xue, H., Chen, S., Bryers, J. D., & Jiang, S. (2009). Zwitterionic carboxybetaine polymer surfaces and their resistance to long-term biofilm formation. *Biomaterials,* 30(28), 5234-5240.

685 Clinton, F. (1975). Sodium cyanoborohydride—a highly selective reducing agent for organic
686 functional groups. *Synthesis,* 3, 135-146.

687 Coughlin, M. L., Liberman, L., Ertem, S. P., Edmund, J., Bates, F. S., & Lodge, T. P. (2021).
688 Methyl cellulose solutions and gels: Fibril formation and gelation properties. *Progress in*
689 *Polymer Science,* 112, 101324.

690 Darvey, I. G., & Ralston, G. B. (1993). Amino acid titration curves-misshapen or mislabeled?
691 *Trends in biochemical sciences,* 18(3), 69-71.

692 Debayle, M., Balloul, E., Dembele, F., Xu, X., Hanafi, M., Ribot, F., Monzel, C., Coppey, M.,
693 Fragola, A., & Dahan, M. (2019). Zwitterionic polymer ligands: an ideal surface coating
694 to totally suppress protein-nanoparticle corona formation? *Biomaterials,* 219, 119357.

695 Dong, Y., Mosquera-Giraldo, L. I., Taylor, L. S., & Edgar, K. J. (2016). Amphiphilic cellulose
696 ethers designed for amorphous solid dispersion via olefin cross-metathesis.
697 *Biomacromolecules,* 17(2), 454-465.

698 Dong, Y., Mosquera-Giraldo, L. I., Troutman, J., Skogstad, B., Taylor, L. S., & Edgar, K. J.
699 (2016). Amphiphilic hydroxyalkyl cellulose derivatives for amorphous solid dispersion
700 prepared by olefin cross-metathesis. *Polymer Chemistry,* 7(30), 4953-4963.

701 Eguchi, N., Kawabata, K., & Goto, H. (2017). Electrochemical polymerization of 4, 4-dimethyl-
702 2, 2'-bithiophene in concentrated polymer liquid crystal solution. *Journal of Materials*
703 *Science and Chemical Engineering,* 5(2), 64-70.

704 Elschner, T., Lüdecke, C., Kalden, D., Roth, M., Löffler, B., Jandt, K. D., & Heinze, T. (2016).
705 Zwitterionic cellulose carbamate with regioselective substitution pattern: a coating
706 material possessing antimicrobial activity. *Macromolecular Bioscience,* 16(4), 522-534.

707 Evans, D., Pye, G., Bramley, R., Clark, A., Dyson, T., & Hardcastle, J. (1988). Measurement of
708 gastrointestinal pH profiles in normal ambulant human subjects. *Gut,* 29(8), 1035-1041.

709 Gabriel, L., Gericke, M., & Heinze, T. (2019). Modular synthesis of non-charged and ionic xylan
710 carbamate derivatives from xylan carbonates. *Carbohydrate polymers,* 207, 782-790.

711 Ganta, S., Devalapally, H., Shahiwala, A., & Amiji, M. (2008). A review of stimuli-responsive
712 nanocarriers for drug and gene delivery. *Journal of Controlled Release,* 126(3), 187-204.

713 Gosecki, M., Setälä, H., Virtanen, T., & Ryan, A. J. (2021). A facile method to control the phase
714 behavior of hydroxypropyl cellulose. *Carbohydrate polymers,* 251, 117015.

715 Haag, S. L., & Bernards, M. T. (2017). Polyampholyte hydrogels in biomedical applications.
716 *Gels,* 3(4), 41.

717 Harijan, M., & Singh, M. (2022). Zwitterionic polymers in drug delivery: A review. *Journal of*
718 *Molecular Recognition,* 35(1), e2944.

719 Haro-Mares, N. B., Meza-Contreras, J. C., López-Dellamary Toral, F. A., González-Cruz, R.,
720 Silva-Guzmán, J. A., & Manríquez-González, R. (2020). A Simplified Method of
721 synthesis to obtain zwitterionic cellulose under mild conditions with active ionic
722 moieties. *Molecules,* 25(13), 3065.

723 Heacock, R., & Marion, L. (1956). The infrared spectra of secondary amines and their salts.
724 *Canadian Journal of Chemistry,* 34(12), 1782-1795.

Heinze, D., Mang, T., Popescu, C., & Weichold, O. (2016). Effect of side chain length and degree of polymerization on the decomposition and crystallization behaviour of chlorinated poly (vinyl ester) oligomers. *Thermochimica Acta,* 637, 143-153.

Kanzian, T., Nigst, T. A., Maier, A., Pichl, S., & Mayr, H. (2009). Nucleophilic reactivities of primary and secondary amines in acetonitrile. *European Journal of Organic Chemistry,* 2009(36), 6379-6385.

Kaßner, L., Kronawitt, J., Klimm, D., Seifert, A., & Spange, S. (2019). Molecular aspects on the amino acid-mediated sol–gel process of tetramethoxysilane in water. *Journal of Sol-Gel Science and Technology,* 90, 250-262.

Kumar, R. A., Vizhi, R. E., Sivakumar, N., Vijayan, N., & Babu, D. R. (2012). Crystal growth, optical and thermal studies of nonlinear optical γ-glycine single crystal grown from lithium nitrate. *Optik,* 123(5), 409-413.

Laschewsky, A. (2014). Structures and synthesis of zwitterionic polymers. *Polymers,* 6(5), 1544-1601.

Laschewsky, A., & Rosenhahn, A. (2018). Molecular design of zwitterionic polymer interfaces: searching for the difference. *Langmuir,* 35(5), 1056-1071.

Laureano-Anzaldo, C. M., Robledo-Ortíz, J. R., & Manríquez-González, R. (2021). Zwitterionic cellulose as a promising sorbent for anionic and cationic dyes. *Materials Letters,* 300, 130236.

Liu, H., Taylor, L. S., & Edgar, K. J. (2015). The role of polymers in oral bioavailability enhancement; a review. *Polymer,* 77, 399-415.

Liu, S., Liu, J., Esker, A. R., & Edgar, K. J. (2016). An efficient, regioselective pathway to cationic and zwitterionic N-heterocyclic cellulose ionomers. *Biomacromolecules,* 17(2), 503-513.

Ma, C., Zhou, H., Wu, B., & Zhang, G. (2011). Preparation of polyurethane with zwitterionic side chains and their protein resistance. *ACS applied materials & interfaces,* 3(2), 455-461.

Mary, Y. S., Ushakumari, L., Harikumar, B., Varghese, H. T., & Panicker, C. Y. (2009). FT-IR, FT-raman and SERS spectra of L-proline. *Journal of the Iranian Chemical Society,* 6(1), 138-144.

Matsumura, K., & Hyon, S.-H. (2009). Polyampholytes as low toxic efficient cryoprotective agents with antifreeze protein properties. *Biomaterials,* 30(27), 4842-4849.

Michels, L., Martin, E., Klaver, P., Edden, R., Zelaya, F., Lythgoe, D. J., Lüchinger, R., Brandeis, D., & O'Gorman, R. L. (2012). Frontal GABA levels change during working memory. *PloS one,* 7(4), e31933.

Mosquera-Giraldo, L. I., Borca, C. H., Meng, X., Edgar, K. J., Slipchenko, L. V., & Taylor, L. S. (2016). Mechanistic design of chemically diverse polymers with applications in oral drug delivery. *Biomacromolecules,* 17(11), 3659-3671.

Nichols, B. L., Chen, J., Mischnick, P., & Edgar, K. J. (2020). Selective oxidation of 2-hydroxypropyl ethers of cellulose and dextran: simple and efficient introduction of versatile ketone groups to polysaccharides. *Biomacromolecules,* 21(12), 4835-4849.

Pasparakis, G., & Tsitsilianis, C. (2020). LCST polymers: Thermoresponsive nanostructured assemblies towards bioapplications. *Polymer,* 211, 123146.

Rodriguez, A. K., Ayyavu, C., Iyengar, S. R., Bazzi, H. S., Masad, E., Little, D., & Hanley, H. J. (2018). Polyampholyte polymer as a stabiliser for subgrade soil. *International Journal of Pavement Engineering,* 19(6), 467-478.

Rosado, M. T., Duarte, M. L. T., & Fausto, R. (1998). Vibrational spectra of acid and alkaline glycine salts. *Vibrational Spectroscopy,* 16(1), 35-54.

Saboo, S., Mugheirbi, N. A., Zemlyanov, D. Y., Kestur, U. S., & Taylor, L. S. (2019). Congruent release of drug and polymer: A "sweet spot" in the dissolution of amorphous solid dispersions. *Journal of Controlled Release,* 298, 68-82.

Samuels, R. J. (1969). Solid-state characterization of the structure and deformation behavior of water-soluble hydroxypropylcellulose. *Journal of Polymer Science Part A-2: Polymer Physics,* 7(7), 1197-1258.

Schram, C. J., Beaudoin, S. P., & Taylor, L. S. (2015). Impact of polymer conformation on the crystal growth inhibition of a poorly water-soluble drug in aqueous solution. *Langmuir,* 31(1), 171-179.

Schram, C. J., Taylor, L. S., & Beaudoin, S. P. (2015). Influence of polymers on the crystal growth rate of felodipine: correlating adsorbed polymer surface coverage to solution crystal growth inhibition. *Langmuir,* 31(41), 11279-11287.

Shen, H., Akagi, T., & Akashi, M. (2012). Polyampholyte nanoparticles prepared by self-complexation of cationized poly (γ-glutamic acid) for protein carriers. *Macromolecular Bioscience,* 12(8), 1100-1105.

Silva, P. J. (2020). New insights into the mechanism of Schiff base synthesis from aromatic amines in the absence of acid catalyst or polar solvents. *PeerJ Organic Chemistry,* 2, e4.

Smith, B. (2019). Organic nitrogen compounds V: Amine salts. *Spectroscopy,* 34(9), 30–37.

Smith, B. C. (2018). The carbonyl group, part V: Carboxylates—Coming clean. *Spectroscopy,* 33(5), 20–23.

Song, J. W., Lee, J. H., Bornscheuer, U. T., & Park, J. B. (2014). Microbial synthesis of medium-chain α, ω-dicarboxylic acids and ω-aminocarboxylic acids from renewable long-chain fatty acids. *Advanced Synthesis & Catalysis,* 356(8), 1782-1788.

Stevens, R. V., Chapman, K. T., & Weller, H. N. (1980). Convenient and inexpensive procedure for oxidation of secondary alcohols to ketones. *The Journal of Organic Chemistry,* 45(10), 2030-2032.

Strätz, J., Liedmann, A., Heinze, T., Fischer, S., & Groth, T. (2020). Effect of sulfation route and subsequent oxidation on derivatization degree and biocompatibility of cellulose sulfates. *Macromolecular Bioscience,* 20(2), 1900403.

Tzianabos, A., Wang, J. Y., & Kasper, D. L. (2003). Biological chemistry of immunomodulation by zwitterionic polysaccharides. *Carbohydrate Research,* 338(23), 2531-2538.

Vamecq, J., Feutelais, Y., Maurois, P., Sghaier, M., Dichi, E., German-Fattal, M., Herrenknecht, C., Gressens, P., Cecchelli, R., & Dehouck, L. (2009). Engineering a GABA endowed with pharmacological CNS activity when given by an extracerebral route. *Medicinal Chemistry Research,* 18(4), 255-267.

Wang, J., Sun, H., Li, J., Dong, D., Zhang, Y., & Yao, F. (2015). Ionic starch-based hydrogels for the prevention of nonspecific protein adsorption. *Carbohydrate polymers,* 117, 384-391.

Wang, R.-M., Zheng, S.-R., & Zheng, Y.-P. G. (2011). *Polymer Matrix Composites and Technology*: Elsevier.

Weißenborn, E., & Braunschweig, B. (2019). Hydroxypropyl cellulose as a green polymer for thermo-responsive aqueous foams. *Soft Matter,* 15(13), 2876-2883.

Wilson, V., Lou, X., Osterling, D. J., Stolarik, D. F., Jenkins, G., Gao, W., Zhang, G. G., & Taylor, L. S. (2018). Relationship between amorphous solid dispersion in vivo absorption and in vitro dissolution: phase behavior during dissolution, speciation, and membrane mass transport. *Journal of Controlled Release,* 292, 172-182.

Wilson, V. R., Lou, X., Osterling, D. J., Stolarik, D. F., Jenkins, G. J., Nichols, B. L., Dong, Y., Edgar, K. J., Zhang, G. G., & Taylor, L. S. (2020). Amorphous solid dispersions of enzalutamide and novel polysaccharide derivatives: Investigation of relationships between polymer structure and performance. *Scientific reports,* 10(1), 18535.

Zeng, R., Guo, K., Wang, Z., Tu, M., Zhao, J., & Wang, J. (2012). Synthesis and self-assembly of biomimetic phosphorylcholine-bound chitosan derivatives. *Reactive and Functional Polymers,* 72(10), 745-751.

Zhang, C., Chao, L., Zhang, Z., Zhang, L., Li, Q., Fan, H., Zhang, S., Liu, Q., Qiao, Y., & Tian, Y. (2021). Pyrolysis of cellulose: Evolution of functionalities and structure of bio-char versus temperature. *Renewable and Sustainable Energy Reviews,* 135, 110416.

Zhang, J., & Zografi, G. (2000). The relationship between "BET" and "free volume"-derived parameters for water vapor absorption into amorphous solids. *Journal of pharmaceutical sciences,* 89(8), 1063-1072.

Zhang, R., & Edgar, K. J. (2015). Water-soluble aminocurdlan derivatives by chemoselective azide reduction using NaBH4. *Carbohydrate polymers,* 122, 84-92.

Zhang, Y., Luo, C., Wang, H., Han, L., Wang, C., Jie, X., & Chen, Y. (2016). Modified adsorbent hydroxypropyl cellulose xanthate for removal of Cu2+ and Ni2+ from aqueous solution. *Desalination and Water Treatment,* 57(56), 27419-27431.

Zheng, L., Sun, Z., Li, C., Wei, Z., Jain, P., & Wu, K. (2017). Progress in biodegradable zwitterionic materials. *Polymer Degradation and Stability,* 139, 1-19.

Zheng, L., Sundaram, H. S., Wei, Z., Li, C., & Yuan, Z. (2017). Applications of zwitterionic polymers. *Reactive and Functional Polymers,* 118, 51-61.

Zhou, Y., & Edgar, K. J. (2022). Regioselective synthesis of polysaccharide–amino acid ester conjugates. *Carbohydrate polymers,* 277, 118886.

Zhou, Y., Petrova, S. P., & Edgar, K. J. (2021). Chemical synthesis of polysaccharide–protein and polysaccharide–peptide conjugates: A review. *Carbohydrate polymers,* 274, 118662.

Zhou, Y., Zhai, Z., Yao, Y., Stant, J. C., Landrum, S. L., Bortner, M. J., Frazier, C. E., & Edgar, K. J. (2022). Oxidized hydroxypropyl cellulose/carboxymethyl chitosan hydrogels permit pH-responsive, targeted drug release. *Carbohydrate polymers,* 300, 120213.